Effective and Accurate Approach for Measuring Key Parameters in Triboelectric Nanogenerators

Luca Fachechi, Laura Blasi, Vincenzo Mariano Mastronardi, Massimo De Vittorio, *Senior Member, IEEE*, and Maria Teresa Todaro

***Abstract*— Triboelectric nanogenerators (TENGs) exploit the triboelectricity of several materials/structures together with an appropriate device architecture to harvest mechanical energy. These devices usually present high output voltages, high internal impedance, and low output currents, and as oscilloscopes are limited by relatively low input impedance, their analysis requires specific instrumentation for the assessment of the main key figures of merit. Due to the increased research interest on this topic, the development of electronic circuits for a rapid and accurate evaluation of the TENGs performances has become urgent. Here, we propose the development of an electronic circuit implemented on a small footprint printed circuit board (PCB) board. This circuit is based on a differential amplifier probe scheme and is a compact and cost-effective approach able to measure both the TENGs outputs: open-circuit voltage at a very high resistive load and short circuit current. Additionally, it offers the possibility to measure voltages under different high resistive loads allowing the assessment of the power behavior of the device. To prove the effectiveness of this approach, triboelectric devices based on carboxymethyl cellulose (CMC) porous aerogel films have been fabricated and analyzed. Furthermore, experimental results in terms of short-circuit currents have been compared with those obtained by using a commercial low noise current amplifier. This approach allows to rapidly and accurately evaluate the behavior of a specific triboelectric device and to effectively compare devices having different characteristics, thus accelerating the development and applications of TENGs.**

***Index Terms*— Current measurement, differential amplifier, electronic circuit, energy harvesting, nanogenerators, triboelectricity, voltage measurement.**

Manuscript received 8 May 2023; revised 12 September 2023; accepted 11 October 2023. Date of publication 30 October 2023; date of current version 14 November 2023. This work was supported in part by the U.S. Department of Commerce under Grant 123456. The Associate Editor coordinating the review process was Dr. Roman Sotner. *(Luca Fachechi and Laura Blasi are co-first authors.) (Corresponding authors: Luca Fachechi; Laura Blasi.)*

Luca Fachechi is with the Istituto Italiano di Tecnologia (IIT), Center for Biomolecular Nanotechnologies, 73010 Arnesano, Lecce, Italy (e-mail: luca.fachechi@iit.it).

Laura Blasi is with the CNR-IMM Istituto per la Microelettronica ed i Microsistemi, UOS di Lecce Via Monteroni c/o Campus Universitario Ecotekne-Palazzina A3, 73100 Lecce, Italy, and also with the Istituto Italiano di Tecnologia (IIT), Center for Biomolecular Nanotechnologies, 73010 Arnesano, Lecce, Italy (e-mail: laura.blasi@cnr.it).

Vincenzo Mariano Mastronardi is with the Dipartimento di Ingegneria dell'Innovazione, Università del Salento, 73100 Lecce, Italy, and also with the Istituto Italiano di Tecnologia (IIT), Center for Biomolecular Nanotechnologies, 73010 Arnesano, Lecce, Italy (e-mail: vincenzomariano.mastronardi@unisalento.it).

Massimo De Vittorio is with the Istituto Italiano di Tecnologia (IIT), Center for Biomolecular Nanotechnologies, 73010 Arnesano, Lecce, Italy, and also with the Dipartimento di Ingegneria dell'Innovazione, Università del Salento, 73100 Lecce, Italy (e-mail: massimo.devittorio@iit.it).

Maria Teresa Todaro is with the Istituto di Nanotecnologia of CNR, Strada Provinciale Lecce-Monteroni—Campus Ecotekne, 73100 Lecce, Italy, and also with the Istituto Italiano di Tecnologia (IIT), Center for Biomolecular Nanotechnologies, 73010 Arnesano, Lecce, Italy (e-mail: mariateresa.todaro@nanotec.cnr.it).

Digital Object Identifier 10.1109/TIM.2023.3328701

I. Introduction

IN THE last decade, due to the fossil fuels energy issues, there is a strong interest in the development of technologies able to exploit renewable energy sources [1], such as geothermal, solar, wind, water flow, and biofuels to promote sustainable development. The progress in science and technology together with the evolution of the modern society has pushed the market of the consumer electronics, promoting the research in the field of microelectronics for the development of more performing, small size and portable microdevices. In this context, novel and sustainable power sources, harvesting energy from the environment for supplying microdevices and self-powered systems, are required. These energy harvesters could replace the electrochemical batteries or complex wiring for powering microsystems and overcome issues related to their employment and environmental impact, including limited lifetime, periodic replacement, and disposal. Among energy sources, mechanical energy is a renewable and sustainable resource widely available in the environment in various forms, including vibration, human motion, walking, mechanical triggering, rotating tire, wind, and flowing water. In recent years, due to the nanotechnology advances, a new class of power sources has been developed, the nanogenerators, able to capture mechanical energy and convert it into electrical energy. The nanogenerators mainly exploit the piezoelectricity or the triboelectricity to capture energy from the environment. The piezoelectricity is the ability of a class of materials, the piezoelectric materials, to exhibit charges on the surfaces as effect of an applied strain [2]. The triboelectricity mechanism arises from the periodic physical contact, i.e., compression and friction, between two materials with different electron affinities [3]. When two triboelectric layers are in contact, charges are redistributed on the internal surfaces of the two materials. During the release mode, a dipole moment is created resulting in a potential difference between the two electrodes: in this condition, there is a flow of charges from one electrode to another until a condition of equilibrium is reached, thus creating electrostatically induced charges on the electrodes. When the triboelectric layers are completely released, no charge flows anymore. Again, during the pressing, there is a rupture of equilibrium that induces charges to flow in the opposite direction. By properly engineering the device

architecture, these charges can be harvested and effectively extracted into an external circuit. Nanogenerators based on triboelectricity, in their four modes of operation [4], have been demonstrated to be effective for harvesting mechanical energy from the environment due to their simple structure, high conversion efficiency, and low cost. Various applications of triboelectric nanogenerators (TENGs) have been successfully demonstrated [5], since 2012 when the first organic materials-based TENGs [6] have been proposed, and this research field is expected to expand in the near future [7].

Actually in nature, there are structures that allow living plants to harvest energy by the triboelectric effect, such as leaves moved by wind [8], thus widening triboelectric energy research interest. Typical key figures of merit of such devices are the open-circuit voltage (V_{OC}), the short-circuit current (I_{SC}), and the generated power. V_{OC} and I_{SC} are experimentally measured using laboratory instruments, while the power behavior is estimated by measuring the voltage or the current under different external resistive loads to extract the maximum power under a matched load. There are some issues related to the measurements of TENGs. These devices usually present a high internal impedance, high voltages, and low output currents [9], [10]. Typically, TENG voltages are measured by a digital oscilloscope, even if the internal impedance of these devices is above the input impedance of most of the commercially available oscilloscopes. This results in output signal strongly attenuated. Indeed, this measurement configuration limits the resistive load applied to the device under test (DUT) up to the impedance of the oscilloscope/passive probe, not enabling the evaluation of the maximum power of the device under matched load.

On the other side, sharp peak short-circuit currents of TENGs can be as low as a few nanoamperes, and they require a current to voltage converter with high gain, so that the converted voltage exceeds the detection limit of the oscilloscopes. For this reason, current measurements on very low loads (i.e., short-circuit currents) require commercially available instruments like SR570 low-noise current preamplifier (LNCP) [11] or VersaSTAT 3 potentiostat [12] or other instrumentation [13].

The development of effective electronic circuits for assessing the main key figures of merit of devices can be helpful to the research community working on TENG energy harvesting.

Here, we propose an electronic circuit, for both current and high impedance voltage measurements, implemented on a (4×2.8) cm^2 printed circuit board (PCB) board, based on a differential amplifier probe scheme. Currently, commercially available measurement equipments (current probes or high impedance voltage probes) are very expensive. There are measurement current circuits, proposed in the literature; however, they are complex, bulky, or do not fully meet requirements for TENG analysis [14]. Our device is compact, cost effective, and able to measure both the TENG outputs: the open-circuit voltage at a very high resistive source and the short-circuit sharp peak current. Additionally, it offers the possibility to measure voltages under different high resistive loads allowing the assessment of the power behavior of the device, as crucial parameter in the analysis of TENGs electrical performance. The developed electronic circuit has been used for the characterization of TENG devices based on carboxymethyl cellulose (CMC) porous aerogel films, and experimental results in terms of currents have been compared with those obtained by using a commercial low-noise current amplifier. This approach allows to rapidly and accurately analyze a specific device and to compare effectively devices with different characteristics, thus accelerating the development and applications of TENGs.

II. Methods

The outputs of TENGs depend on the involved triboelectric materials, the device architecture and size, the magnitude and frequency of the applied forces, and the ambient conditions (temperature and relative humidity). According to the implemented device and measurement conditions, TENG peak voltages can range from a few volts [15] up to hundred volts [16], while output peak currents are typically low, ranging from one hundred of nA [15] to tens of μA [17] for devices of a few cm^2 area. Moreover, TENGs have a relatively high impedance and they deliver maximum power in a range from a few megaohms [16] to hundreds of megaohms [18]. Additionally, current peaks in TENGs can be sharp (microampere in hundreds of microseconds), meaning that the high-frequency components are quite important, and therefore, electronics with wide bandwidth is required.

Fig. 1 reports the developed electronic circuit, implemented on the same PCB board to measure open-circuit voltages and short-circuit currents. Specifically, Fig. 1(a) shows a simplified scheme of the voltage circuit based on a differential voltage amplifier. It has some advantages over the passive probe: the nanogenerator is connected to the ground (GND) through high impedance path, the common mode (CM) voltage is not amplified, and the circuit can be located closely to the DUT using a very short cable. This results in a better electrical isolation of the DUT from noise sources and interferences. Open-circuit voltage measurements usually require a buffer amplifier having a high input impedance because of the high impedance of TENGs and a low output impedance to be coupled to the oscilloscope. The very high TENGs output impedance, often of the order of tens of megaohms, impacts on bandwidth performances of the amplifier, because even input capacitance of a few picofarads limits the bandwidth below few kilohertz. Reducing input capacitance is hard with discrete electronic components; therefore, integrated amplifiers, such as instrumentation amplifiers, are preferred [19]. Additionally, instrumentation amplifiers have high intrinsic capacity to reject CM noise and high-power supply voltage reject ratio, mainly at low frequency. Moreover, the instrumentation amplifier gain can be selected by only one resistor, without resistor trimming requirements. Commercially available instrumentation amplifiers with low noise and high gain-bandwidth product (GBW) have been selected. Finally, wide supply range amplifiers are preferred in order to obtain high dynamic range.

For the voltage circuit, the INA121 amplifier due to its very low input differential capacitance (1 pF), low input CM

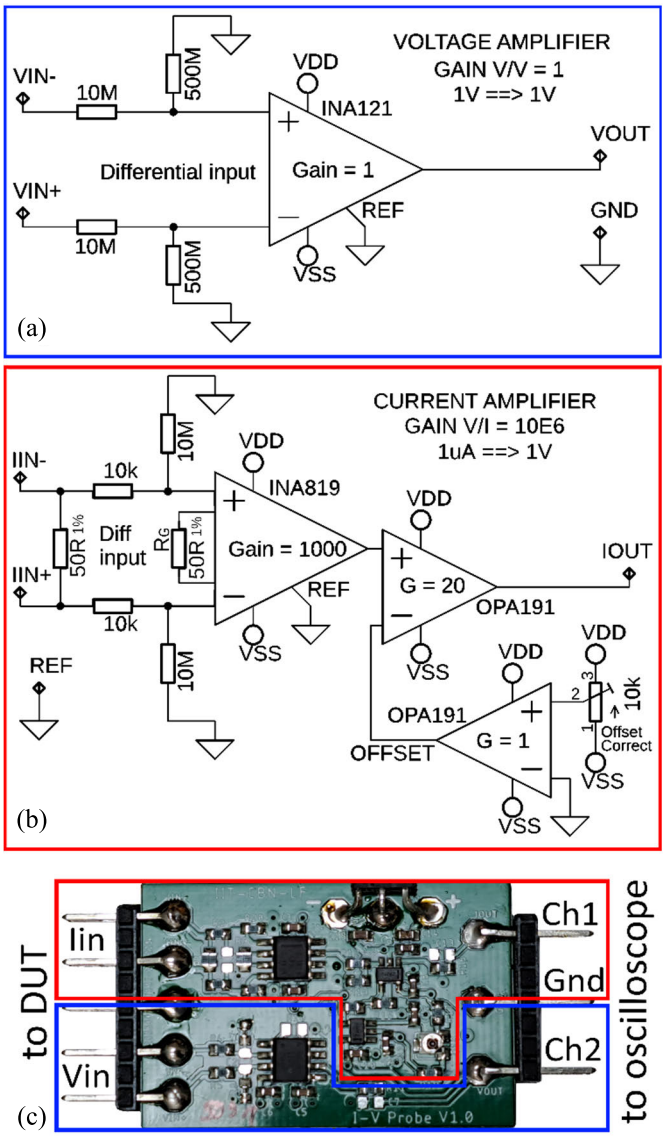

Fig. 1. Developed circuit with (a) simplified scheme of the voltage circuit, (b) simplified scheme of the current circuit, and (c) two circuits implemented on a PCB board.

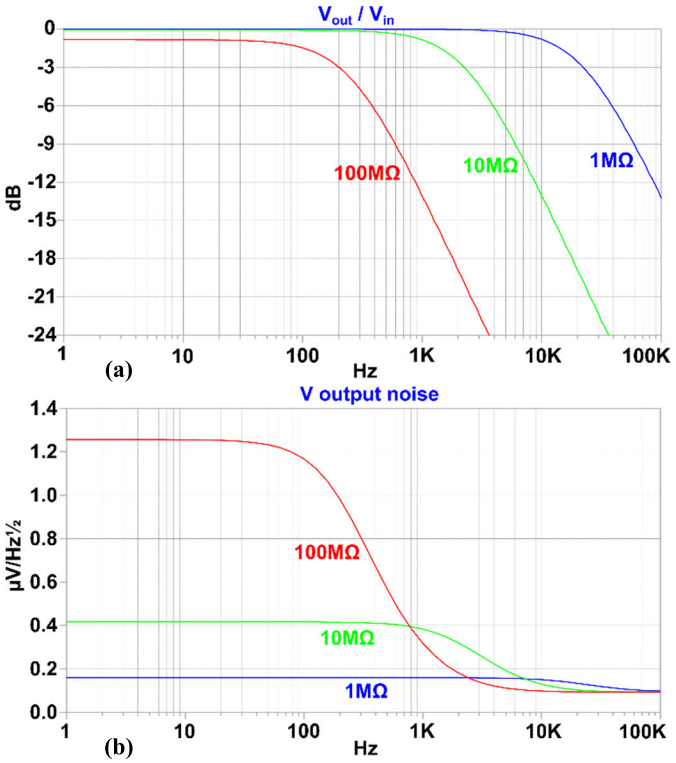

Fig. 2. Simulation results of (a) frequency response of the output voltage versus the input voltage and (b) noise spectral density under different input source resistances (100, 10, and 1 MΩ).

capacitance (12 pF), and very low bias current (4 pA) has been chosen.

The amplifier gain has been settled to 1, as the triboelectric device voltage level is enough high to be measured by the oscilloscope without amplification. Furthermore, surrounding passive components have been chosen to obtain an input differential impedance of 1 GΩ.

To verify the performances of the voltage circuit, ac analysis and noise analysis have been performed by LTSpice.

Fig. 2 shows the simulation results of the alternating current (AC) and noise analysis under different input source resistances (100, 10, and 1 MΩ). Fig. 2(a) reports the frequency response of the output voltage versus the input voltage. At low frequencies, the magnitude of this signal decreases by increasing the input resistance down to an attenuation factor of 0.91 for 100-MΩ source resistance. At the same time, the bandwidth reduces from 23 kHz to 230 Hz applying higher source resistances. Indeed, bandwidth reduction is mainly due to the input INA121 capacitances in series with the high output impedance of the DUT, whereas INA121 bandwidth (600 kHz at unity gain) does not impact on the whole circuit bandwidth. Bench measurements have been performed, thus confirming simulation results.

Fig. 2(b) shows the noise spectral density under different input source resistances. The noise increases when the input source resistance increases due to the source resistance thermal noise. The simulated total root mean square output voltage (V_{RMS}) noise is 38 μV.

Fig. 1(b) shows the simplified scheme of the current circuit based on a differential voltage instrumentation amplifier. The differential configuration, as for the voltage circuit, results in a better isolation of the device from external noise and interferences.

Short-circuit current measurements usually require amplifiers with high gain, because a few ohms (usually 50 Ω) resistance input shunt resistor is used to generate a voltage signal at the amplifier input. In this case, the amplifier input capacitance can be neglected; however, due to the high-voltage gain, the input offset voltage becomes relevant and a supplementary stage is exploited to compensate output voltage offset.

The implemented circuit has an input shunt resistance of 50 Ω, the same used in commercial current amplifiers. Due to the low current values, the current circuit consists of two amplification stages, the first with a voltage gain of 1000 and the second one with a voltage gain of 20, to obtain a voltage

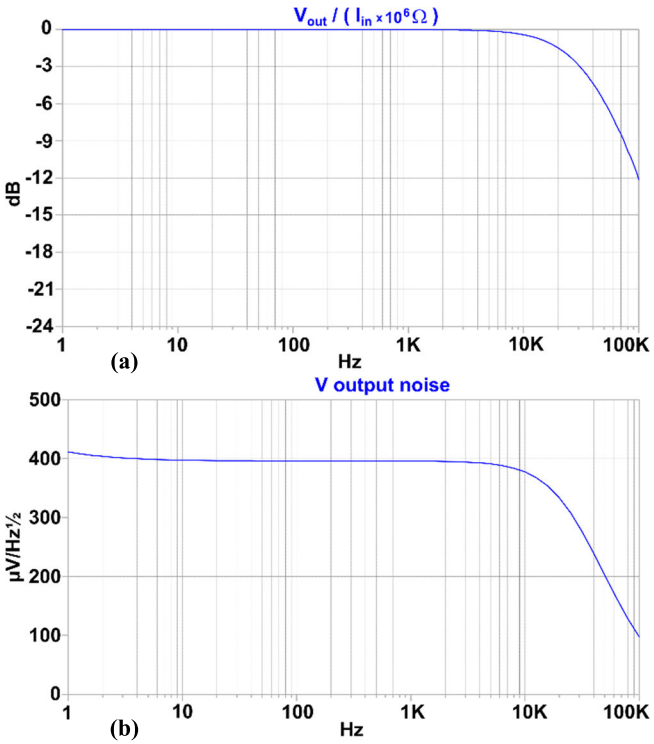

Fig. 3. Simulation results of (a) frequency response of the output voltage versus the input current and (b) voltage output noise spectral density with input shunt resistor of 50 Ω.

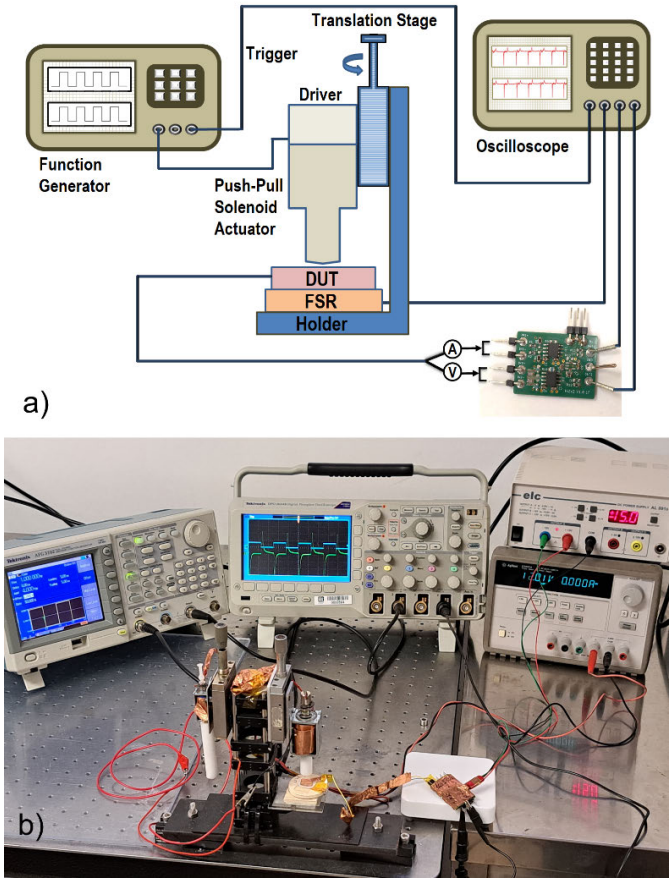

Fig. 4. (a) Schematic representation and (b) picture of the measurement setup used to evaluate the output response of the TENGs as effect of the pressing-release excitation. The open-circuit voltage and the short-circuit current are measured by exploiting the developed circuit, through the corresponding connection pins. Outputs of the developed circuit are connected to the oscilloscope.

to current conversion factor of 10^6. The circuit bandwidth is limited only by the bandwidth of the first stage amplifier.

In the proposed current circuit, INA819 amplifier has been selected because of its very low noise and high GBW (2 MHz at unity gain and 30 kHz at gain 1000).

Fig. 3 reports the simulation results of the ac and noise analysis of the current circuit with an input shunt resistor of 50 Ω. Fig. 3(a) shows the frequency response of the output voltage versus the input current taking into account the conversion factor of 10^6. The bandwidth of the whole circuit results to be 30 kHz (because the INA819 bandwidth) to meet the features of sharp current peaks for this class of devices. Fig. 3(b) shows the noise spectral density with a simulated total output V_{RMS} noise of 77 mV.

Both the voltage and current circuits have been implemented on a compact PCB board having (4 × 2.8) cm^2 size [Fig. 1(c)]. Exploiting the proposed circuit, the measurements of open-circuit voltage on a very high resistive load (1 GΩ) and short-circuit current (50 Ω) can be performed. Additionally, it offers the possibility to measure voltages under different high resistive loads allowing the assessment of the power behavior of the DUT. The whole circuit implemented on the PCB board is a cost-effective approach, with an expenditure below 40 €.

III. Experiment

Several TENG device architectures and materials have been proposed and implemented to harvest energy in an efficient way. The device proposed in this study consists of two materials with different electron affinities, where a porous structure of a triboelectric positive material is filled with a triboelectric negative material. The TENG configuration is in contact-separation mode and the device is gapless. Despite TENG devices without air gap provide poor electrical output performance, the absence of the gap results in an easier fabrication process and enables large-scale fabrication, thus opening the way for novel applications in energy harvesting and sensing.

The proposed nanogenerator consists of a porous CMC aerogel film impregnated with poly(dimethyl siloxane) (PDMS) and embedded into two thin PDMS films. The obtained multilayer structure has been sandwiched by two Al foils for electrical connections. CMC porous aerogel film has been prepared starting from an aqueous solution (1.5% concentration), which has been freeze-dried and compressed. Then, the CMC film aerogel has been filled by a PDMS solution under a vacuum-assisted process. PDMS films have been spin-coated on both sides.

The CMC/PDMS multilayer structure film has been cut into 1 cm^2 area dies and devices have been electrically connected. A custom measurement setup has been built up for TENG nanogenerator analysis to perform pressing-release measurements in the vertical direction.

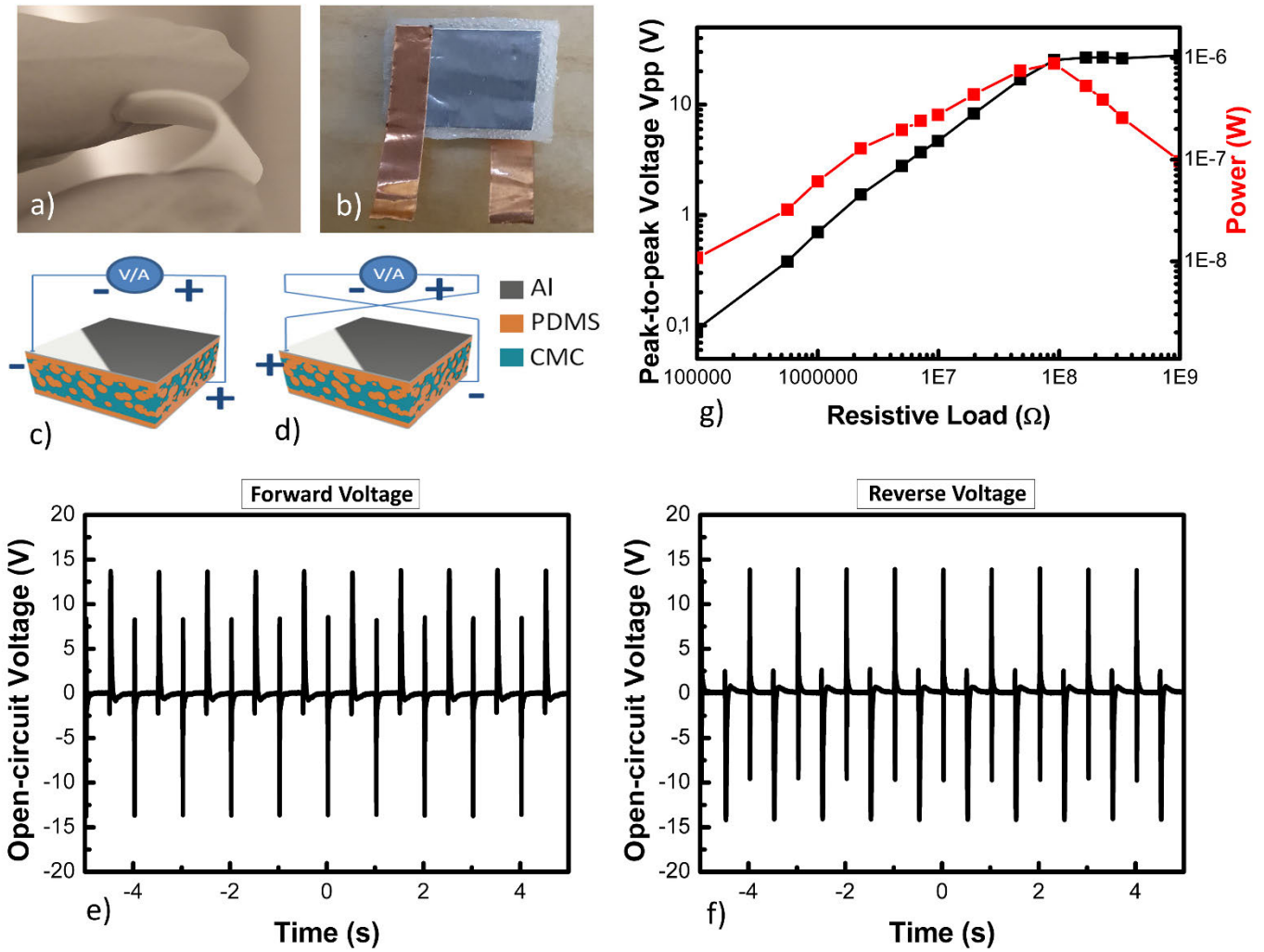

Fig. 5. Output open-circuit voltage and power estimation under different external resistive loads. (a) Image of a fabricated CMC/PDMS multilayer structure. (b) Image of a photograph of the developed triboelectric device. (c) Schematic representation of the forward connection. (d) Schematic representation of the reverse connection. (e) Output open-circuit voltage in forward connection (time scale: 10 s). (f) Output open-circuit voltage in reverse connection (time scale: 10 s). (g) Peak-to-peak voltage (left) and generated power (right) under different resistive loads.

Fig. 4(a) shows a schematic representation of the setup, whereas Fig. 4(b) is a picture of the experimental setup.

A push–pull solenoid actuator mounted on a vertical translation stage has been employed to provide forces in the range of 1–10 N. The solenoid is driven by a square wave provided by a function generator (dual-channel function generator AFG3102 by Tektronix). The actuator driver circuit is a controlled switch based on a power n-MOSFET, where its gate is directly connected to the function generator. The DUT is connected to the developed circuit implemented on the PCB board for either voltage or current measurements. This circuit has been connected to the Tektronix DPO2024B digital oscilloscope for output measurements.

To apply consistent experimental measurement conditions [20], a test bed has been implemented. All tests were performed applying a periodic force to the device (5 N) at a frequency of 1 Hz in ambient conditions (18 °C and 50% relative humidity). To assess the applied forces, a commercial force sensing resistor has been employed (FSR400 by Pololu) and the calibration curve (resistance versus weight) has been obtained under static conditions in the 20 gr − 1 Kg range. All cables together with the setup measurement components have been shielded to limit electrical noise/interferences from the environment.

IV. Results and Discussion

Based on this setup, voltage measurements have been performed. Fig. 5(a) and (b) reports the representative images of the realized nanogenerators. Fig. 5(a) shows the fabricated CMC/PDMS multilayered structure where can be noticed its high flexibility and mechanical resistance. Fig. 5(b) reports a picture of the developed triboelectric device, where for electrical measurements, adhesive stripes of Cu have been used. Devices have been analyzed in forward and reverse connections, as schematically represented in Fig. 5(c) and (d). Fig. 5(e) and (f) shows the output voltage (V_{OC}) response of the TENG nanogenerator in the forward and reverse

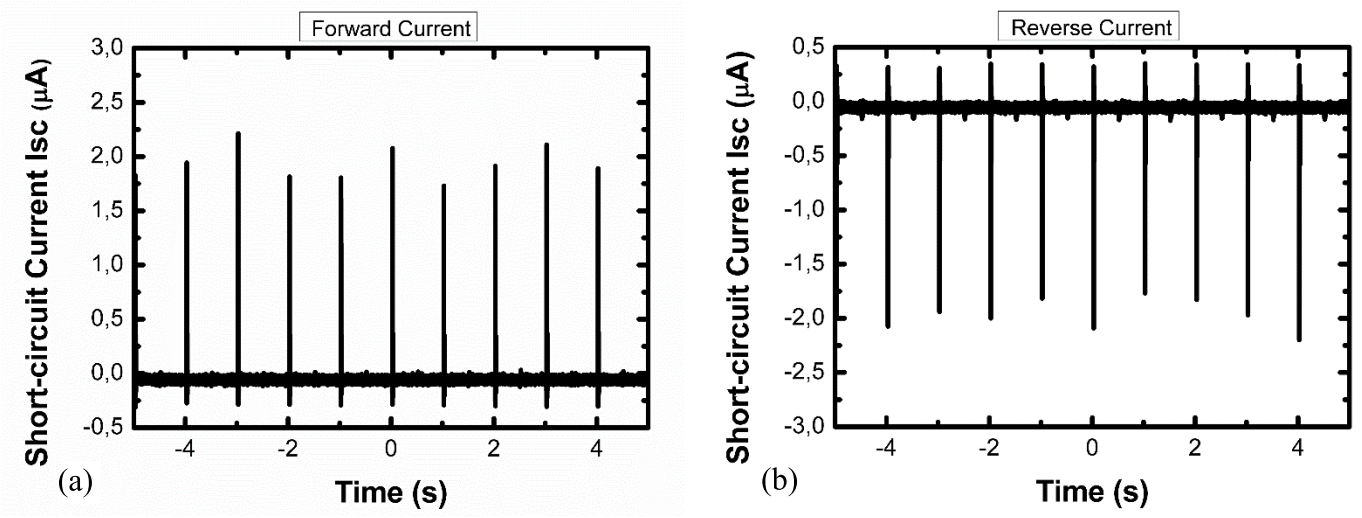

Fig. 6. Output short-circuit current signals under (a) forward and (b) reverse connections (time scale: 10 s) acquired by using the proposed electronic circuit.

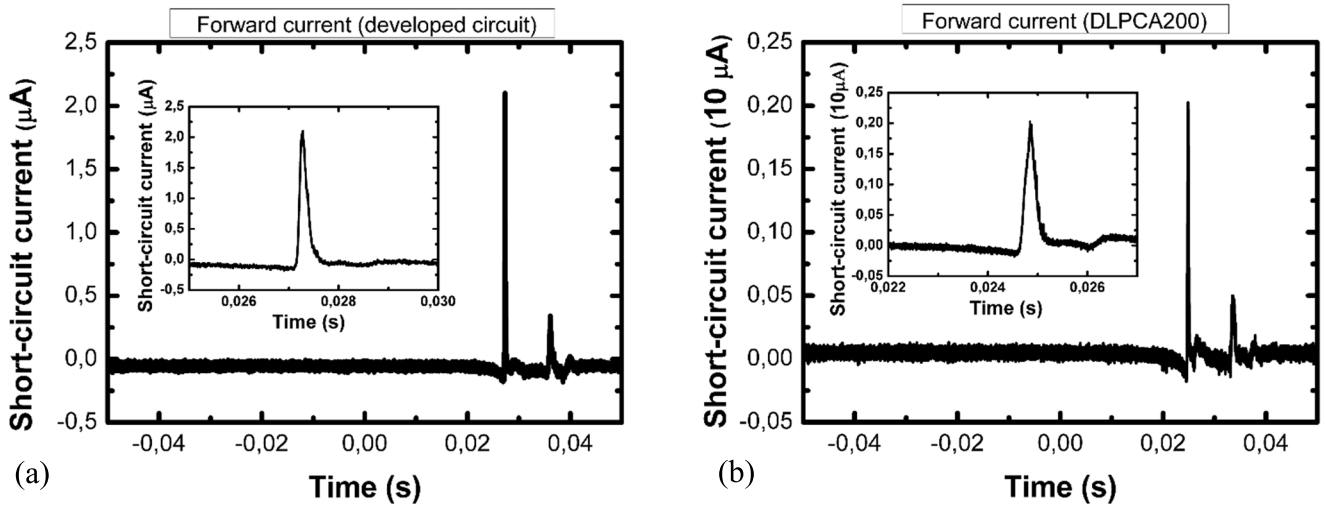

Fig. 7. Output short-circuit current signals acquired by (a) developed circuit and (b) commercial low-noise current amplifier (DLPCA-200) on a 100 ms time scale. Insets show a magnified view of the same plots.

connections, respectively. The signals were acquired on a 10 s time scale for both configurations. The output voltage signals have almost the same profile, and voltage peaks repeat identically after each cycle of pressing release.

The peak-to-peak voltage is 27.8 V and, as shown in the two plots, the signal profiles are reversed in the two configurations, as expected. Fig. 5(g) shows in the same plot the peak-to-peak voltage (left) and the generated power (right) under different resistive external loads. The effective resistive loads are obtained by considering the parallel between the external load with the input resistance of the voltage amplifier. Peak-to-peak voltage enhances by increasing the external load, up to reaching a plateau at very high loads. The generated power results to be up to 0.9 μW when the external resistive load is close to 90 MΩ. This result suggests that the device impedance is around 100 MΩ.

Fig. 6 reports the output short-circuit current signals under forward and reverse connections, acquired in 10 s time scale. The graphs show an important peak during the pressing phase, with a peak-to-peak value around 2.2 μA. The current signal during the release is almost negligible.

To compare the current measurement results obtained with the developed circuit and to validate them, the same devices have been analyzed by using a commercial low noise current amplifier (DLPCA-200 provided by Femto) with a variable gain, bandwidth up to 500 kHz and an input impedance of 50 Ω.

Fig. 7 shows the short-circuit current measurements performed by means of the developed circuit having a gain of 10^6 V/A [Fig. 7(a)] and by using DLPCA200 amplifier with a selected gain of 10^5 V/A [Fig. 7(b)]. The time scale has been chosen as low as 100 ms to highlight the features of the current peaks. The insets show a zoom view of the same graphs. The peaks appear very similar and sharp with a pulse height of 2 μA and a pulsewidth below 0.5 ms. Both amplifiers show almost the same noise level. It can be noticed that the

signal of Fig. 7(b) appears noisier simply because of the lower current to voltage gain.

The peak-to-peak current is around 2.2 μA, in agreement with the results reported in Fig. 6, where plots were acquired with larger time scale.

V. Conclusion

Electronic circuits able to assess the main key figures of merit of TENG nanogenerators represent powerful tools for a rapid and at the meantime accurate analysis. In this article, we proposed a compact and cost-effective electronic circuit, based on a differential amplifier probe scheme, implemented on a (4 $\times$ 2.8) cm^2 PCB board, which enables TENG outputs measurements in terms of open-circuit voltage at a very high resistive source and short-circuit current. Furthermore, it allows voltage measurements under different high resistive external loads to assess the power behavior. This circuit has been developed taking into account critical issues proper of triboelectric devices. To prove the effectiveness of this approach, TENG devices based on CMC porous aerogel films have been fabricated and analyzed. Additionally, current signals have been compared with those obtained by using a commercial low-noise current amplifier. This approach could open the way for a rapid and accurate analysis of TENG nanogenerators with different characteristics, thus accelerating the development and applications of this class of devices.

Acknowledgment

The authors would like to thank Mr. G. Branca from Branca s.a.s. in Montesano Salentino (LE) for its technical help in choosing thermohydraulic components for building up the vacuum system.

References

[1] F. Sher, O. Curnick, and M. T. Azizan, "Sustainable conversion of renewable energy sources," *Sustainability*, vol. 13, no. 5, p. 2940, Mar. 2021.

[2] M. T. Todaro et al., "Piezoelectric MEMS vibrational energy harvesters: Advances and outlook," *Microelectron. Eng.*, vols. 183–184, pp. 23–36, Nov. 2017.

[3] S. S. Indira, C. A. Vaithilingam, K. S. P. Oruganti, F. Mohd, and S. Rahman, "Nanogenerators as a sustainable power source: State of art, applications, and challenges," *Nanomaterials*, vol. 9, no. 5, p. 773, May 2019.

[4] A. Ahmed et al., "Integrated triboelectric nanogenerators in the era of the Internet of Things," *Adv. Sci.*, vol. 6, no. 24, Dec. 2019, Art. no. 1802230.

[5] W.-G. Kim et al., "Triboelectric nanogenerator: Structure, mechanism, and applications," *ACS Nano*, vol. 15, no. 1, pp. 258–287, 2021.

[6] F.-R. Fan, Z.-Q. Tian, and Z. Lin Wang, "Flexible triboelectric generator," *Nano Energy*, vol. 1, no. 2, pp. 328–334, Mar. 2012.

[7] T. Cheng, Q. Gao, and Z. L. Wang, "The current development and future outlook of triboelectric nanogenerators: A survey of literature," *Adv. Mater. Technol.*, vol. 4, no. 3, Mar. 2019, Art. no. 1800588.

[8] F. Meder, A. Mondini, and B. Mazzolai, "Measuring triboelectric energy conversion in leaves of living plants," *IEEE Instrum. Meas. Mag.*, vol. 25, no. 9, pp. 4–9, Dec. 2022.

[9] R. Walden, C. Kumar, D. M. Mulvihill, and S. C. Pillai, "Opportunities and challenges in triboelectric nanogenerator (TENG) based sustainable energy generation technologies: A mini-review," *Chem. Eng. J. Adv.*, vol. 9, Mar. 2022, Art. no. 100237.

[10] S. Lu et al., "Regulating the high-voltage and high-impedance characteristics of triboelectric nanogenerator toward practical self-powered sensors," *Nano Energy*, vol. 87, Sep. 2021, Art. no. 106137.

[11] H. Hwang et al., "Mesoporous highly-deformable composite polymer for a gapless triboelectric nanogenerator via a one-step metal oxidation process," *Micromachines*, vol. 9, no. 12, p. 656, Dec. 2018.

[12] Q. Zheng et al., "Highly porous polymer aerogel film-based triboelectric nanogenerators," *Adv. Funct. Mater.*, vol. 28, no. 13, Mar. 2018, Art. no. 1706365.

[13] Y. J. Kim, J. Lee, S. Park, C. Park, C. Park, and H.-J. Choi, "Effect of the relative permittivity of oxides on the performance of triboelectric nanogenerators," *RSC Adv.*, vol. 7, no. 78, pp. 49368–49373, 2017.

[14] Y. H. Tehrani and S. M. Atarodi, "Design & implementation of high dynamic range current measurement system for IoT applications," *IEEE Trans. Instrum. Meas.*, vol. 71, pp. 1–9, 2022.

[15] M. Beyranvand and A. Gholizadeh, "Facile and low-cost synthesis of flexible nano-generators based on polymeric and porous aerogel materials," *Current Appl. Phys.*, vol. 20, no. 1, pp. 226–231, Jan. 2020.

[16] H.-Y. Mi, X. Jing, M. A. B. Meador, H. Guo, L.-S. Turng, and S. Gong, "Triboelectric nanogenerators made of porous polyamide nanofiber mats and polyimide aerogel film: Output optimization and performance in circuits," *ACS Appl. Mater. Interface*, vol. 10, no. 36, pp. 30596–30606, Sep. 2018.

[17] S. S. K. Mallineni, H. Behlow, Y. Dong, S. Bhattacharya, A. M. Rao, and R. Podila, "Facile and robust triboelectric nanogenerators assembled using off-the-shelf materials," *Nano Energy*, vol. 35, pp. 263–270, May 2017.

[18] J. Chun et al., "Mesoporous pores impregnated with au nanoparticles as effective dielectrics for enhancing triboelectric nanogenerator performance in harsh environments," *Energy Environ. Sci.*, vol. 8, no. 10, pp. 3006–3012, 2015.

[19] T. N. Lin, B. Wang, and A. Bermak, "Review and analysis of instrumentation amplifier for IoT applications," in *Proc. IEEE 61st Int. Midwest Symp. Circuits Syst. (MWSCAS)*, vol. 2018, Aug. 2018, pp. 258–261.

[20] D. Hong, Y.-M. Choi, and J. Jeong, "Test bed for contact-mode triboelectric nanogenerator," *Rev. Sci. Instrum.*, vol. 89, no. 6, Jun. 2018, Art. no. 065110.

Luca Fachechi is a Researcher with the Center for Biomolecular Nanotechnologies (CBN) of the Istituto Italiano di Tecnologia (IIT), Lecce, Italy. His current research focuses on sensors powered by vibrational harvested energy by means of piezoelectric and triboelectric transducers and on the development of electronic front end for sensors. He has long expertise in electronic hardware design and firmware implementation, as well as wireless sensor networks.

Laura Blasi received the master's degree in biology from the University of Ferrara, Ferrara, Italy, in 1999, and the Ph.D. degree in innovative materials and technologies from the National Nanotechnology Laboratory of the University of Salento, Lecce, Italy, in 2006.

Currently, she is a Researcher with the CNR-IMM, Lecce. Her research activities are focused on nanobiotechnology, in particular on the realization of biomimetic scaffolds for tissue engineering and regeneration and on the development and characterization of biomimetic surfaces for lab-on-a-chip applications.

Vincenzo Mariano Mastronardi received the M.S. degree in ingegneria delle telecomunicazioni from the Università del Salento, Lecce, Italy, in 2012, and the Ph.D. degree in material science and technology from the Center for Biomolecular Nanotechnologies, Istituto Italiano di Tecnologia (IIT), Lecce, in 2016, and the High Qualified Research Doctor degree in nanotechnologies and nanostructured innovative materials from Scuola Interpolitecnica di Dottorato (SIPD), Turin, Italy.

From 2016 to 2021, he was a Post-Doctoral with the Center for Biomolecular Nanotechnologies, IIT. Since 2022, he is a Researcher with the Department of Innovation Engineering of Università del Salento, Lecce. His research interests include wearable and inertial sensors, flexible and silicon-based microelectromechanical systems (MEMS), and piezoelectric energy harvester devices.

Massimo De Vittorio (Senior Member, IEEE) is a Coordinator of the Center for Biomolecular Nanotechnologies of the Istituto Italiano di Tecnologia, Lecce, Italy, and a Full Professor with the Università del Salento, Lecce, where he is a Lecturer of the courses "electronics for biomedical applications" and "nanotechnologies for electronics." He has been responsible for more than ten years of the nanodevice division at the National Nanotechnology Laboratory (NNL) of the CNR Istituto Nanoscienze. His research activity deals with the development of science and technology applied to nanophotonics, nanoelectronics, and nano- and microelectromechanical systems (NEMS/MEMS) for applications in the fields of life science, energy, and information and communication technologies (ICT).

Maria Teresa Todaro received the M.S. degree in electronic engineering from the Politecnico di Bari, Bari, Italy, in 2000, and the Ph.D. degree in materiali e tecnologie innovative from the Università di Lecce, Lecce, Italy, in 2004.

In 2005, she was a Post-Doctoral Researcher with the University College of Cork, Cork, Ireland. Currently, she is a Researcher with the Istituto di Nanotecnologia of the Consiglio Nazionale delle Ricerche, Lecce. Her research interests include piezoelectric materials, micro- and nanofabrication, flexible and silicon-based microelectromechanical systems (MEMS), sensors and actuators, piezoelectric, and triboelectric energy harvesting devices.

Open Access funding provided by 'Istituto Italiano di Tecnologia' within the CRUI CARE Agreement